Photoic crystal nanobeam cavity devices for on-chip integrated silicon photonics

Daquan Yang, Xiao Liu, Xiaogang Li, Bing Duan, Aiqiang Wang, and Yunfeng Xiao

Citation: D Q Yang, X Liu, X G Li, B Duan, A Q Wang, and Y F Xiao, Photoic crystal nanobeam cavity devices for on−chip integrated silicon photonics[J]. *J. Semicond.*, 2021, 42(2).
View online: https://doi.org/10.1088/1674−4926/42/2/023103

REVIEWS

Journal of Semiconductors
(2021) 42, 023103
doi: 10.1088/1674-4926/42/2/023103

Photoic crystal nanobeam cavity devices for on-chip integrated silicon photonics

Daquan Yang[1, †], Xiao Liu[1], Xiaogang Li[1], Bing Duan[1], Aiqiang Wang[1], and Yunfeng Xiao[2, 3, 4, 5, †]

[1]State Key Laboratory of Information Photonics and Optical Communications, and School of Information and Communication Engineering, Beijing University of Posts and Telecommunications, Beijing 100876, China

[2]State Key Laboratory for Artificial Microstructure and Mesoscopic Physics, School of Physics, Peking University, Beijing 100871, China

[3]Frontiers Science Center for Nano-Optoelectronics & Collaborative Innovation Center of Quantum Matter, Beijing 100871, China

[4]Collaborative Innovation Center of Extreme Optics, Shanxi University, Taiyuan 030006, China

[5]Beijing Academy of Quantum Information Sciences, Beijing 100193, China

Abstract: Integrated circuit (IC) industry has fully considered the fact that the Moore's Law is slowing down or ending. Alternative solutions are highly and urgently desired to break the physical size limits in the More-than-Moore era. Integrated silicon photonics technology exhibits distinguished potential to achieve faster operation speed, less power dissipation, and lower cost in IC industry, because their COMS compatibility, fast response, and high monolithic integration capability. Particularly, compared with other on-chip resonators (*e.g.* microrings, 2D photonic crystal cavities) silicon-on-insulator (SOI)-based photonic crystal nanobeam cavity (PCNC) has emerged as a promising platform for on-chip integration, due to their attractive properties of ultra-high *Q*/*V*, ultra-compact footprints and convenient integration with silicon bus-waveguides. In this paper, we present a comprehensive review on recent progress of on-chip PCNC devices for lasing, modulation, switching/filting and label-free sensing, etc.

Key words: PCNC; integrated silicon photonics; More-than-Moore; lab-on-a-chip; hybrid devices

Citation: D Q Yang, X Liu, X G Li, B Duan, A Q Wang, and Y F Xiao, Photoic crystal nanobeam cavity devices for on-chip integrated silicon photonics[J]. *J. Semicond.*, 2021, 42(2), 023103. http://doi.org/10.1088/1674-4926/42/2/023103

1. Introduction

Over the past few decades, the mainstream of integrated circuit (IC) industry has been mainly powered by Moore's Law, which is targeted at achieving faster operation speed, less power dissipation, and lower cost[1]. The key driving force behind Moore's Law is the ongoing MOSFET scaling down to nanoscales[2, 3]. As shown in Fig. 1(a), the number of transistors that can be purchased per dollar is increasing, but since 2012 it almost encounters a bottleneck. Correspondingly, the feature size of the transistor is significantly reduced at first, but slowly decreasing to the order of ~10 nm in 2017. However, this trend is beginning to bump up against the fundamental physical limits on their size, which means the approaching end of the Moore's Law. As shown in Fig. 1(b), the final International Semiconductor Technology Roadmap (ITRS) report predicts transistor scaling will end in 2021 and clearly states that it will no longer follow the path of decreasing process nodes after 10 nm[4, 5].

In fact, Moore's Law is a techno-economic model that has enabled the information technology industry to double the performance and functionality of digital electronics roughly every two years within a fixed cost, power, and area[6]. Fig. 2(a) shows that the main technological development trends will follow two paths in the More-than-Moore era. The first path we call "More than Moore", is from the function, to achieve multi-functional expansion of the circuit. Another path we call "More Moore" is to continue to increase the density of integrated circuits through the miniaturization of devices. However, because traditional materials are difficult to break through their own limits, we may further promote the development of integrated circuits through the research and development of new materials, new structures, and new principle devices, and eventually move toward three-dimensional (3D) chip stacks integration[7, 8]. Different and revolutionary strategies and approaches are highly and urgently needed to meet the requirements of faster, cheaper, and more energy efficient in the More-than-Moore era. So far, silicon photonics technology exhibits distinguished potential and has become one of the leading technological solutions for integrated photonics that target applications such as data centers, telecommunications, and high-performance computing (HPC)[9]. As shown in Fig. 2(b), its total market size will increase dramatically in these fields. Approaching the opportunity of large scale marketization, silicon photonics have drawn intensive attention, driven by its advantages, market demand, and national strategy.

Silicon photonics have been widely investigated in recent years, which benefits from academic research efforts and available commercial complementary metal–oxide–semiconductor (CMOS) process for potential mass-production applications[10–12]. Versatile passive- and active-silicon-based nanophotonic devices have been proposed for applications includ-

Correspondence to: D Q Yang, Email: ydq@bupt.edu.cn; Y F Xiao, yfxiao@pku.edu.cn

Received 27 MAY 2020; Revised 6 AUGUST 2020.

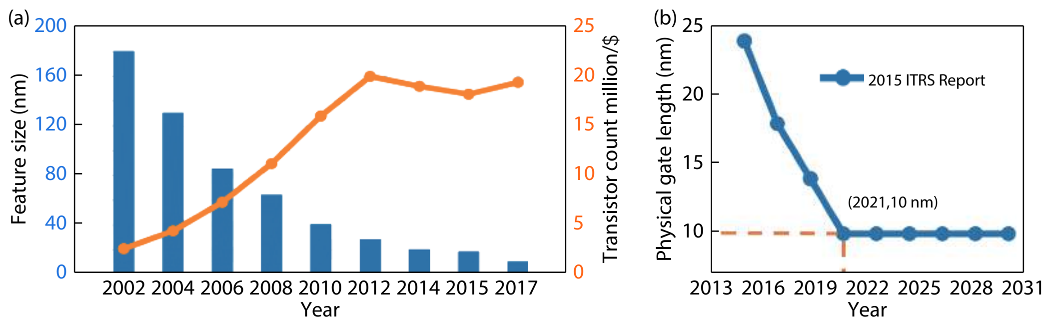

Fig. 1. (Color online) (a) Number and size of transistors bought per dollar. Source: The end of Moore's law. The Economist, April, 2015. (b) The ITRS most recent report predicts transistor scaling will end in 2021. Source: International Semiconductor Technology Roadmap (ITRS).

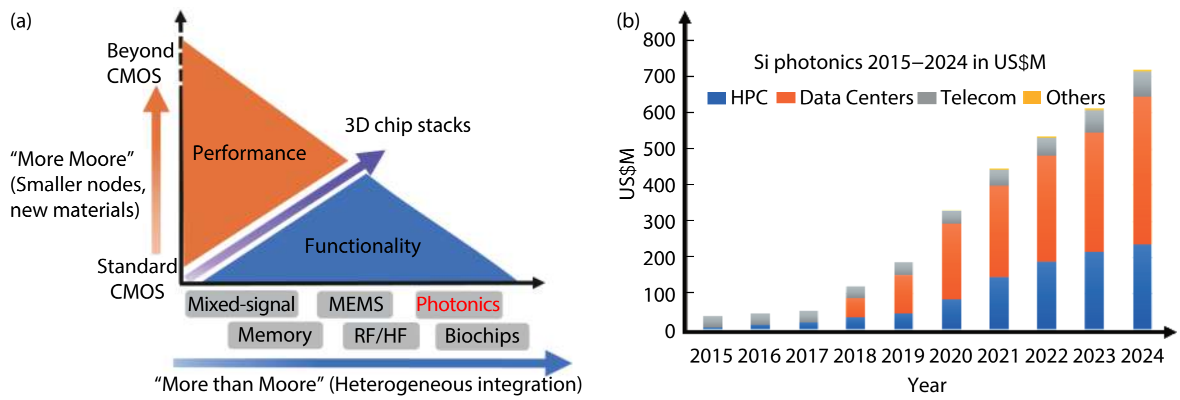

Fig. 2. (Color online) (a) The development trend of the semiconductor industry in the More-than-Moore Era. Source: International Semiconductor Technology Roadmap (ITRS). (b) Silicon photonics 2015–2024 market forecast. Source: Silicon Photonics Report Yole Développement.

ing optical interconnects, optical routers, remote telecommunications, modulation, and sensing. However, there are some challenging tasks need to be solved, including the intrinsic properties limits of pure silicon and the CMOS fabrication compatibility for on-chip silicon sources[10]. Recently researchers have reported the integrated stimulated Raman scattering silicon lasers[13], germanium-on-silicon lasers[14], and hybrid III–V on silicon lasers[15], but there are some problems, such as undesirably high optical external pumping, insufficient lasing emission, and complicated fabrication process. Hybridizing silicon waveguides and resonators/cavities with active materials have been considered as an alternative solution for lasing emission, optical modulation, and detection. This hybrid integration on silicon has shown potential advantages because of its low cost, easy processing, and various active materials[16]. Many investigations about the hybrid integration on silicon have been demonstrated, including semiconductor nanotubes[17], superconducting nanowires[18], polymers[19], single III–V semiconductor nanowires[20], transition-metal dichalcogenides (TMDs)[21] or graphene[22]. In terms of the view, the natural host photonic structures of active materials deposited or grown on silicon are microcavities, because of their high quality factors (Q) and low mode volumes (V)[23, 24]; therefore, large Q/V is helpful for laser threshold reduction, ultralow voltage and energy-efficient optical modulation and ultra-sensitive label-free sensing.

Particularly, photonic crystal nanobeam cavity (PCNC) is considered as an ideal platform for on-chip integration, due to the advantages of an ultracompact footprint, enhanced light–matter interactions, high integrability with optical waveguides/circuits, and compatibility with CMOS processes[25, 26]. To date, various optical devices based on PCNC have been demonstrated, such as optical lasers, optical modulators, optical switches/filters, and label-free sensors. By incorporating these photonic devices, versatile and reconfigurable photonic networks can be realized. Thus, PCNC-based devices in near infrared wavelengths could be potentially significant for future on-chip integrated silicon photonics. In this review, we will focus on photonics devices based on PCNCs.

2. On-chip PCNC devices for lasing

Photonic crystal lasers, with large Q/V, have enhanced photon emission below threshold through the Purcell effect, and can operate at a higher modulation speed[27]. Compared with two-dimensional (2D) photonic crystal slabs, the PCNCs with exceptional Q/V in a much smaller footprint have attracted particular interest. So far, PCNC lasers based on various materials have been demonstrated using different nanobeam cavities[27–40], as summarized in Fig. 3. Insets show the device structures, materials, and threshold power, respectively. It can be found that III–V semiconductor compounds (gallium arsenide, GaAs and indium phosphide, InP) with high electron mobility have proved extremely successful for the realization of lasers. However, the major problems of III–V semiconductor compounds are high cost and poor CMOS compatibility, which limits its further development for on-chip integrated photonics application. Compared with III–V semiconductors compounds, CMOS-compatible SOI-based photonics devices are a promising platform for realizing low cost and high density on-chip integrated photonics. However, silicon cannot pro-

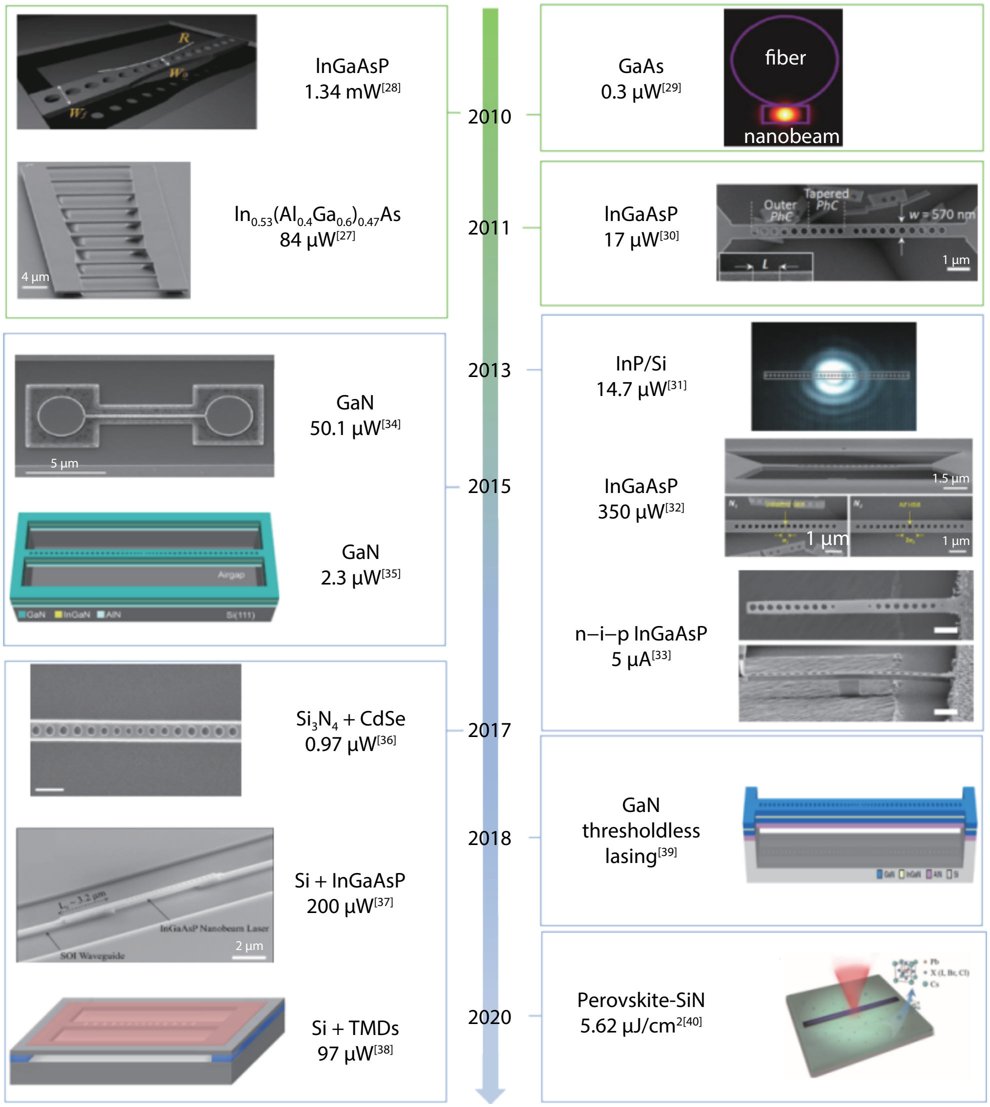

Fig. 3. (Color online) A summary of PCNC lasers (2010–2018). Insets show the device structures, materials, and threshold power, respectively.

duce light directly due to its natural indirect band gap. Hence, recently silicon-based hybrid laser platforms, such as using high-performance III–V and 2D materials attached to silicon, have attracted much attention[37, 38].

For example, Lee *et al.* demonstrated an ultracompact nanobeam laser by effectively integrating a wavelength-scale unidirectional III–V materials onto a SOI waveguide[37], as shown in Fig. 4(a). The light from the III–V laser was initially coupled to the III–V waveguide, and was connected to one end of the nanolaser. The light was then vertically coupled from the upper III–V waveguide to the lower SOI waveguide via a directional coupler in the overlapping region of the III–V waveguides and the SOI waveguides. At last, the light from the nanolaser propagated along the low-loss silicon waveguide[37]. The SEM of the proposed III–V/Si nanobeam laser was shown in Fig. 4(b). It is worth mentioning that the coupling efficiency between the InGaAsP nanolaser and conventional SOI waveguide reached ~83%. The lasing started at a threshold pump power of ~0.2 mW, and the wavelength was 1556 nm in Fig. 4(c). It has demonstrated an efficient hybrid integration of a wavelength-scale photonic crystal nanolaser and a SOI waveguide. This nanoscale hybrid III–V/Si laser is considered as a promising platform for future compact, faster, and efficient silicon nanophotonics[37].

Monolayer transition-metal dichalcogenides (TMDs) exhibit great potential to be the smallest and efficient optical gain media for low energy-consumption nanolasers due to its strong excitonic emission[38, 41]. For example, Ning *et al.* firstly demonstrated the use of a silicon PCNCs and a monolayer TMD to generate a room-temperature laser operation in the infrared region[38], as shown in Fig. 5(a). This was mainly due to the unique combination of a TMD monolayer with a silicon-transparent wavelength emission, and a high-*Q* silicon PCNC. Fig. 5(b) described the lasing emission spectrum under different pump power. As the pump power increased, it showed clearly the appearance of strong lasing peaks at 1052 nm of the first mode and 1132 nm of the second mode. To represent the lasing characteristics more accurately in Fig. 5(c), PL spectrum was measured at increasing pump levels, showing a clear lasing emission peak at 1132 nm and a very low lasing threshold ~ 97 μW. Moreover, the lasing *Q*-factor could be extracted from the data in Fig. 5(c) and this was the highest *Q*-factor of any 2D TMD-based laser reported so far. The SOI-based PCNCs would be considered as very attractive for integrated silicon nanophotonics at the wavelength transparent to silicon[38]. Adding only a monolayer of non-silicon

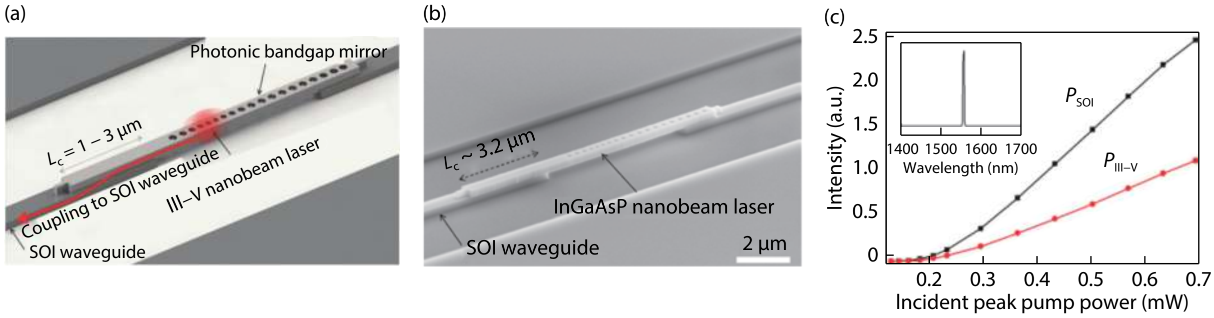

Fig. 4. (Color online) (a) Schematic and (b) SEM of the proposed hybrid III–V/Si nanolaser attached to a conventional silicon-on-insulator (SOI) waveguide. (c) Measured output power near the end of the SOI waveguide (black) and near the InGaAsP nanobeam (red) against incident peak pump power. The inset shows a lasing emission spectrum near 1550 nm.

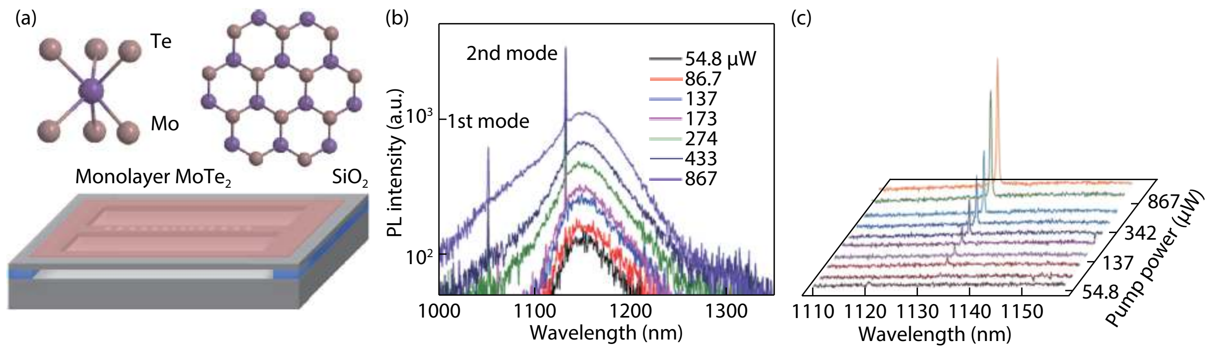

Fig. 5. (Color online) (a) Schematic of the proposed room temperature, suspended silicon nanobeam laser with a monolayer $MoTe_2$ on top. The corresponding lasing spectra of the nanobeam laser under different pump power levels (b) using a grating resolution: 150 g/mm (0.41 nm), and (c) using a grating resolution: 600 g/mm (0.09 nm).

material may be the closest approach to a silicon laser as ever possible, which opens opportunities for CMOS process integration. The unique combination structure of $MoTe_2$–nanobeam cavity can possibly be used for 2D TMD-based electrically driven lasers via electrical injection[33], and thus is a promising platform for optical communications.

3. On-chip PCNC devices for modulation

Silicon photonics technology is poised to resolve short reach interconnects, and optical modulators are essential for such an interconnect. In addition, Pockels effect[42], Kerr effect[43] and the Franz–Keldysh effect[44] are the main electric-optic (EO) effects that cause electric absorption or electric refraction. In order to realize the optical modulator, one method is based on changing the optical properties of the waveguide medium (i.e. refractive index or optical absorption) through linear EO effect[45, 46] or free-carrier dispersion[47, 48]. Another method is to control the properties of the waveguide medium by adopting an optical pumping, thereby actuating the nonlinear optical phenomena in the waveguide[49].

Several parameters have been used to characterize the performance of EO modulator: footprint, modulation voltage, modulation speed, extinction ratio, and energy consumption. So far, various silicon hybrid EO modulators have been achieved. But for waveguide-based modulators, they have large footprints and high-power consumptions due to the interaction lengths about several tens of micrometers[22, 50]. The micro-ring resonator (MRR)-based modulators increase bending loss and decrease Q factor, resulting in high power consumption and low modulation efficiency[51, 52]. Recently, PCNC has been extensively used as EO modulators due to its excellent properties namely ultrasmall footprints and convenient integration with bus-waveguides. However, due to the absorbed distortion caused by carrier dispersion and the difficulty of direct PN doping in silicon nanobeam structures. Therefore, it is necessary to hybrid integrate with emerging materials, such as 2D materials, lithium niobate, EO polymers etc. In particular, the 2D materials and lithium niobate integrated on silicon platform are becoming fully CMOS-compatible. Existing PCNC-based EO modulators have been proposed including those based on a Si-graphene hybrid[53, 54], a Si-organic hybrid[55, 56], and a Si–lithium niobate hybrid[57, 58]. Here, several works are listed in Table 1 in chronological order. This predicts that tremendous efforts have been made towards realizing smaller size and high-performance optical modulators by hybrid integrating with new materials.

We can find that many works based on the combination of PCNC and new materials have been reported[46, 53, 60]. Especially, graphene as an active medium is attracting interest because of its high carrier mobility[61] and gate-controllable broadband absorption[62]. All-optical modulator has been theoretically proposed by using the strong Kerr effect of graphene with PCNC[49]. However, the feasibility of these works is demonstrated through simulation, which makes it a promising candidate for achieving modulators experimentally.

4. On-chip PCNC devices for switching/filting

Optical switch is widely used in optical communicati-

Table 1. Comparison with PCNC-based modulators.

Structure	Material	Device footprint (μm^2)	Modulation voltage (V)	Modulation speed (GHz)	Extinction ratio (dB)	Energy consumption (J/bit)	Year
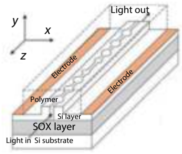	Si-polymer	7.7	0.2	86	13	–	2011[45]
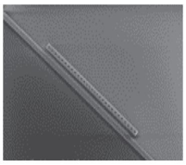	Si	20	0.1	10^{-5}	10	0.5	2013[59]
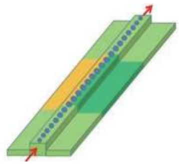	Si	4	0.62	20	6	1.4×10^{-17}	2014[47]
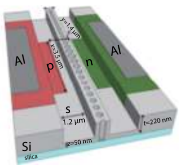	Si	7	1	1.3	3	4.2×10^{-14}	2014[48]
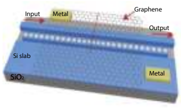	Si-graphene	20	−6.4	133	12.5	6×10^{-13}	2015[53]
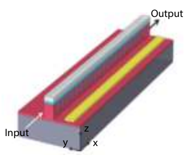	Si-polymer	3.6	1	224	10.9	7.5×10^{-16}	2018[46]
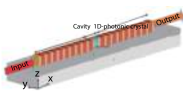	Si- ITO	1.892	0.1	119.89	3.484	5.9×10^{-19}	2019[60]

on[63], optical computing[64], optical interconnect and an optical information processing system[65]. Due to the large capacity of the optical switch array and the high integration of silicon-based chips, the optical switch should have small size and low power consumption. Several structures have been proposed to achieve optical switch, including silicon microring resonators (MRRs)[66] and Mach–Zehnder interferometers (MZIs)[67]. However, the radius of MRR is generally in the order of tens of microns, and the arm length of MZI is also in the order of hundreds of microns or even millimeters. Therefore, the key technology in realizing the optical switch is to reduce the device size and energy loss.

PCNCs are increasingly gaining interest in optical switch due to the advantages of high Q/V. Therefore, it could be an effective method in realizing low power-consumption optical switches. For comparison, Table 2 summarizes the performances of some PCNC-based optical switches. For thermo-optic (TO) switch, Su *et al.* proposed and experimentally demonstrated a 2 × 2 TO crossbar switch based on dual-PCNCs[69]. The cavity resonance wavelength could be red-shifted via thermally perturbing the refractive index of silicon, and then TO switch can be realized. Meanwhile, Su *et al.* proposed a compact 2 × 2 EO switch based on dual PCNCs with identical PN junctions respectively using the same schematic diagram[73]. To realize the EO switch, an external bias voltage was applied on the PN junction. This changed the width of the depletion region, thereby tuning the refractive index of silicon PCNC. Miniature all-optical switches with high-speed and low power attract much attention in communication networks because of its versatility, such as optical logic operation[77], wavelength conversion[78], optical demultiplexing[79], etc. So far, all-optical switch based PCNC has been achieved by several methods, such as using Fano resonance[80], multi-channel switch[75] or silicon-polymer hybrid structure[81]. These works show that all-optical switches have great potential in improving optical information processing capacity and reducing the power consumption of on-chip all-optical signal processing[80].

With the advancement of photonic integration technology, the filters have drawn much attention due to highly energy-efficient tunability[82]. The tunability can be achieved through TO effects[83], electromechanical effects, and opto-electro-mechanical effects[84, 85]. Generally, direct reconfiguration based on TO effect is realized by integrating a microheater on a silicon waveguide[86, 87]. Note that the TO effect is overwhelmingly preferred for high tuning efficiency, a large tun-

Table 2. Comparison with PCNC-based optical switches.

Principle	Structure	Material	Device footprint (μm^2)	Switching power	Extinction ratio (dB)	Insertion loss (dB)	Year
	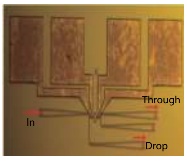	Si	–	1 mW	15	0.66	2016[68]
Thermo-optic effect	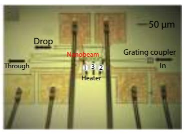	Si	4500	0.16 mW	15	1.5	2017[69]
	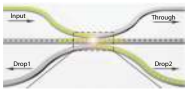	Si	14	–	–	1.5	2020[70]
	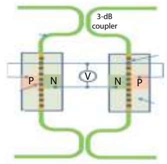	Si	–	474 aJ/bit	–	2	2015[71]
Electro-optic effect	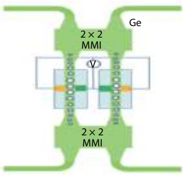	Ge-on-Si_3N_4	–	8 pJ/bit	6	0.97	2016[72]
	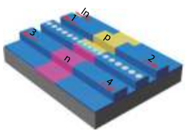	Si	200	2.6 fJ/bit	14.2	1.2	2016[73]
	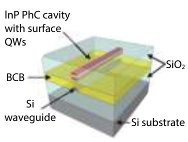	InP	10	6 mW	3.6	–	2014[74]
Kerr nonlinearity	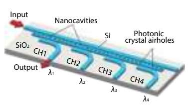	Si	31	1.6 pJ	24	4	2018[75]
	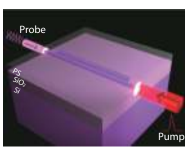	Si+polymer	16	0.76 pJ	–	–	2020[76]

ing range and those requiring simple fabrication based on SOI, due to the high TO coefficient of silicon (1.86×10^{-4} K^{-1}), corresponding the temperature sensitivity of ~80 pm/K[88]. Zhang *et al.* demonstrated a TO tunable filter based on a suspended PCNC shown in Figs. 6(a) and 6(b). We can see that the TO tunability filters possess record high tuning efficiency of 21 nm/mW and the widest tuning range of ~43.9 nm[89], as shown in Fig. 6(c). This device has been considered as an ideal platform for integrated photonics circuits, such as crossbar switches and Bragg grating filters[89], due to the advantages of ultra-high tuning efficiency and rapid response.

5. On-chip PCNC devices for label-free sensing

Ultra-sensitive and label-free detection of the analyte plays an important part in the field of homeland security, environment protection and medical diagnostics[90–93]. Optical microcavities such as whispering gallery mode (WGM) cavities, Fabry–Pérot (F–P) cavities and photonic crystal (PhC) cavities are considered as promising candidates for label-free sensing[94–97]. Particularly, PCNCs have extensively attracted attentions due to the advantages of ultrahigh *Q*/*V*, ultra-small footprint, and excellent CMOS compatibility properties[98].

Hence, most research has focused on the optimization of PCNCs design to improve sensitivity, as shown in Table 3. With the rapid development of technology, micro-nano devices are moving towards high miniaturization and integration. Much research has been proposed for label-free sens-

Table 3. Comparison with PCNC-based optical sensors.

Structure	Material	Sensitivity (nm/RIU)	Q	Detection limit	Year
	Si	83	35000	2 pM	2013[99]
	Si	200	20000	–	2012[100]
	Si	269	27000	–	2012[101]
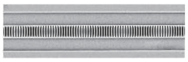	Polymer	386	36000	10 mg/dL	2011[102]
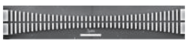	Si	410	~10000	–	2013[103]
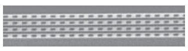	Si	451	7015	10 ag/mL	2014[104]
	InGaAsP	461	~10000	–	2015[105]
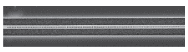	Porous Si	1023	9000	1.6 pm/nM	2019[106]

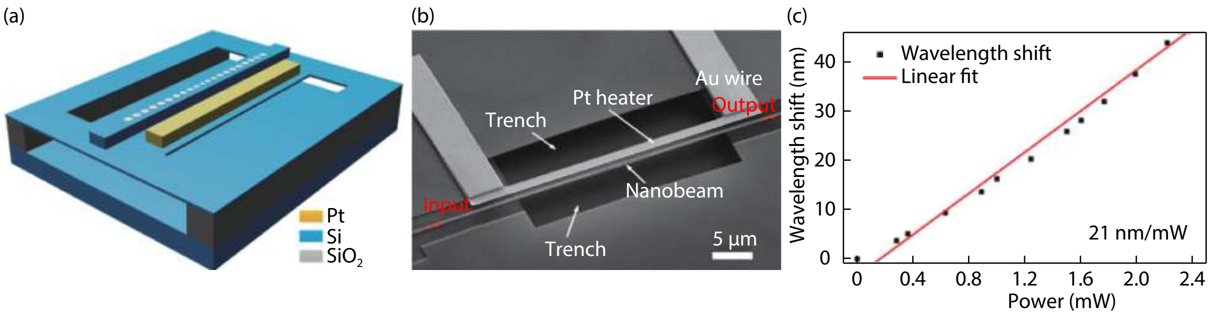

Fig. 6. (Color online) (a) Schematic of the proposed TO tunable nanobeam filter. (b) SEM image of the fabricated PCNC filter. (c) Measured wavelength shifts against heating powers.

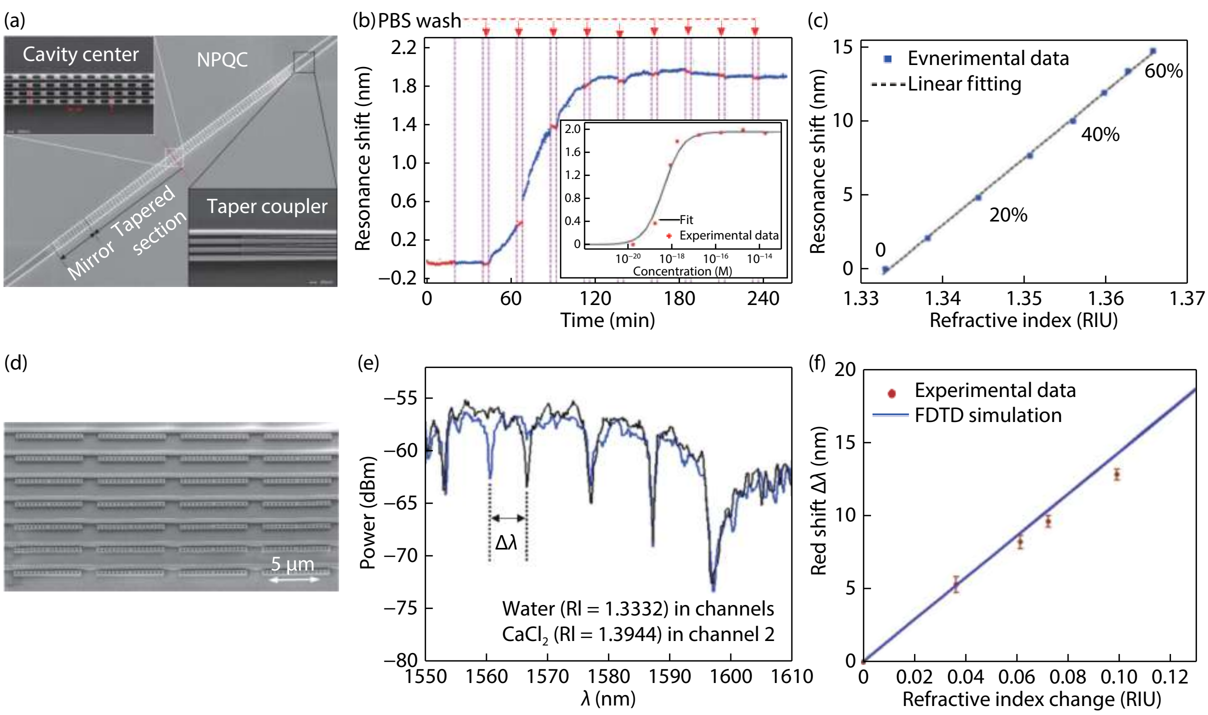

Fig. 7. (Color online) (a) SEM image of the proposed parallel quadrabeam PCNCs. (b) Real-time monitoring of streptavidin/biotin binding. Inset: resonance shift as a function of streptavidin concentration in PBS. (c) Resonance shifts as a function of the refractive indices with different concentrations ethanol/water solutions. (d) SEM of nanoscale sensor array. (e) Red shift of the targeted resonator occurs because of the higher refractive index of the $CaCl_2$ solution. (f) Experimental data showing the redshifts for various refractive index solutions.

ing by integrating microfluidics with PCNCs. For instance, Yang *et al.* presented a nanoslotted parallel quadrabeam photonic crystal cavity sensor, with high sensitivity of 451 nm/RIU and high-Q of 7015 in aqueous environments at wavelength of 1550 nm[104], as shown in Fig. 7(a). They also monitored streptavidin-biotin binding affinity in phosphate buffered saline (PBS) solution and the detection limit is down to 10 ag/mL, as shown in Figs. 7(b) and 7(c). In this configuration, the PDMS microfluidic channel is integrated with PCNC sensors, which provides a promising platform for multiplexing on chip and point-of-care medical diagnostics. In addition, they also show the potential application in single-molecule detection[107]. On the other hand, works integrating multi-channel microfluidic have been proposed for multiplexing sensing. Mandal *et al.* demonstrated a nanoscale optofluidic sensor arrays with multiple channels based on PCNCs, as shown in Fig. 7(d)[108]. To verify sensing ability of the nanoscale optofluidic sensor array, fluidic architecture is embedded in sensor array and achieving the RI resolution of 7×10^{-5}, corresponding to the mass limit of around 35 ag in the measurement of water and $CaCl_2$ solution, as shown in Figs. 7(e) and 7(f)[108]. This research opens the door for the detection sensitivity at the tens of attograms level in the field of label-free sensing and shows the multiplexing capabilities of this architecture.

In conclusion, with the rapid development of silicon photonics devices, higher integration, and miniaturization are required. Among these, PCNCs are considered as candidates for on-chip label-free sensing and multiple channel sensing, due to the advantages of an ultra-small footprint, ultrahigh Q/V, and excellent CMOS compatibility properties[109].

6. Summary

To be implemented in practice, technical challenges are existed in manufacturing. The silicon photonics chip can be fabricated cost-effectively with CMOS-compatible technology. However, the fabrication tolerance limits the practical applications of PCNCs, which makes them impractical for high-yield production. Fabrication tolerance in the position and size of the PhC structures may result in fluctuations of resonance wavelength and Q factor[110], and it also limits the parameter space for sweeping device design[111]. So far, various strategies to improve the fabrication tolerance have been demonstrated, such as using UV-lithography in fabrication[112], allowing precision wavelength trimming of devices[113], controlling the Q by optimizing configurations[114], and using a subwavelength grating (SWG) structure[115]. An ultra-compact PCNC with large fabrication tolerance is desirable for silicon-based photonic integrated circuits and there is a need for further studies and industry efforts to realize outstanding fabrication tolerance.

In this paper, we review recent advances on photonics devices for lasers, modulators, switches/filters, and sensors based on PCNCs. It has been shown that PCNCs with ultrahigh Q/V, ultrasmall footprint are an idea platform for the monolithic integration and extending the capability of these optical devices, in which the key is that the PCNCs can greatly improve light-matter interaction. The optical devices show good characteristics and high-volume production, which are expected to benefit large-scale photonic-integrated circuits on silicon in the near future. Furthermore, photonic integration should not be required to surpass electronic integration, but its unique advantages should be used as a supplement to electronic integration to solve problems that electronic integration cannot solve in the More-than-Moore era.

Acknowledgements

This work was supported by the National Key R&D Program of China (Grant No. 2016YFA0301302 and No. 2018YFB 2200401), the National Natural Science Foundation of China (Grant Nos. 11974058, 11825402, 11654003, 61435001), Beijing Academy of Quantum Information Sciences (Grant No. Y18G20), Key R&D Program of Guangdong Province (Grant No. 2018B030329001), Beijing Nova Program (Grant No. Z201100006820125) from Beijing Municipal Science and Technology Commission, Fundamental Research Funds for the Central Universities (Grant No. 2018XKJC05) and the High Performance Computing Platform of Peking University.

References

[1] Shalf J M, Leland R. Computing beyond Moore's law. Computer, 2015, 48, 14
[2] Liu M S, Liu Y, Wang H J, et al. Design of GeSn-based heterojunction-enhanced N-channel tunneling FET with improved subthreshold swing and ON-state current. IEEE Trans Electron Devices, 2015, 62, 1262
[3] Yue Y Z, Hao Y, Zhang J C, et al. AlGaN/GaN MOS-HEMT with HfO_2 dielectric and Al_2O_3 interfacial passivation layer grown by atomic layer deposition. IEEE Electron Device Lett, 2008, 29, 838
[4] Markov I L. Limits on fundamental limits to computation. Nature, 2014, 512, 147
[5] Wesling P. The Heterogeneous integration roadmap: Enabling technology for systems of the future. 2020 Pan Pacific Microelectronics Symposium (Pan Pacific), 2020, 1
[6] Shalf J. The future of computing beyond Moore's Law. Phil Trans Royal Soc A, 2020, 378, 20190061
[7] Pei J, Deng L, Song S, et al. Towards artificial general intelligence with hybrid Tianjic chip architecture. Nature, 2019, 572, 106
[8] Liu W L, Li M, Guzzon R S, et al. A fully reconfigurable photonic integrated signal processor. Nat Photon, 2016, 10, 190
[9] Thomson D, Zilkie A, Bowers J E, et al. Roadmap on silicon photonics. J Opt, 2016, 18, 073003
[10] Dai D X, Yin Y L, Yu L H, et al. Silicon-plus photonics. Front Optoelectron, 2016, 9, 436
[11] Shi Y C, Chen J Y, Xu H N. Silicon-based on-chip diplexing/triplexing technologies and devices. Sci China Inf Sci, 2018, 61, 080402
[12] Guo J S, Dai D X. Silicon nanophotonics for on-chip light manipulation. Chin Phys B, 2018, 27, 104208
[13] Rong H S, Xu S B, Kuo Y H, et al. Low-threshold continuous-wave Raman silicon laser. Nat Photon, 2007, 1, 232
[14] Sun X C, Liu J F, Kimerling L C, et al. Toward a germanium laser for integrated silicon photonics. IEEE J Sel Top Quantum Electron, 2010, 16, 124
[15] Duan G H, Jany C, Le Liepvre A, et al. Hybrid III–V on silicon lasers for photonic integrated circuits on silicon. IEEE J Sel Top Quantum Electron, 2014, 20, 158
[16] Yang Y C, Gao P, Li L Z, et al. Electrochemical dynamics of nanoscale metallic inclusions in dielectrics. Nat Commun, 2014, 5, 4232
[17] Pyatkov F, Fütterling V, Khasminskaya S, et al. Cavity-enhanced light emission from electrically driven carbon nanotubes. Nat Photon, 2016, 10, 420
[18] Chen B G, Wu H, Xin C G, et al. Flexible integration of free-standing nanowires into silicon photonics. Nat Commun, 2017, 8, 20

[19] Liu J L, Xu G M, Liu F G, et al. Recent advances in polymer electro-optic modulators. RSC Adv, 2015, 5, 15784
[20] Joyce H J, Gao Q, Hoe Tan H, et al. III–V semiconductor nanowires for optoelectronic device applications. Prog Quantum Electron, 2011, 35, 23
[21] Bie Y Q, Grosso G, Heuck M, et al. A $MoTe_2$-based light-emitting diode and photodetector for silicon photonic integrated circuits. Nat Nanotech, 2017, 12, 1124
[22] Liu M, Yin X B, Ulin-Avila E, et al. A graphene-based broadband optical modulator. Nature, 2011, 474, 64
[23] Vahala K J. Optical microcavities. Nature, 2003, 424, 839
[24] Song Q H. Emerging opportunities for ultra-high *Q* whispering gallery mode microcavities. Sci China Phys Mech Astron, 2019, 62, 74231
[25] Deotare P B, McCutcheon M W, Frank I W, et al. High quality factor photonic crystal nanobeam cavities. Appl Phys Lett, 2009, 94, 121106
[26] Quan Q M, Deotare P B, Loncar M. Photonic crystal nanobeam cavity strongly coupled to the feeding waveguide. Appl Phys Lett, 2010, 96, 203102
[27] Zhang Y, Khan M, Huang Y, et al. Photonic crystal nanobeam lasers. Appl Phys Lett, 2010, 97, 051104
[28] Ahn B H, Kang J H, Kim M K, et al. One-dimensional parabolic-beam photonic crystal laser. Opt Express, 2010, 18, 5654
[29] Gong Y Y, Ellis B, Shambat G, et al. Nanobeam photonic crystal cavity quantum dot laser. Opt Express, 2010, 18, 8781
[30] Lu T W, Chiu L H, Lin P T, et al. One-dimensional photonic crystal nanobeam lasers on a flexible substrate. Appl Phys Lett, 2011, 99, 071101
[31] Fegadolli W S, Kim S H, Postigo P A, et al. Hybrid single quantum well InP/Si nanobeam lasers for silicon photonics. Opt Lett, 2013, 38, 4656
[32] Lee P T, Lu T W, Chiu L H. Dielectric-band photonic crystal nanobeam lasers. J Lightwave Technol, 2013, 31, 36
[33] Jeong K Y, No Y S, Hwang Y, et al. Electrically driven nanobeam laser. Nat Commun, 2013, 4, 2822
[34] Niu N, Woolf A, Wang D Q, et al. Ultra-low threshold gallium nitride photonic crystal nanobeam laser. Appl Phys Lett, 2015, 106, 231104
[35] Triviño N V, Butté R, Carlin J F, et al. Continuous wave blue lasing in III-nitride nanobeam cavity on silicon. Nano Lett, 2015, 15, 1259
[36] Yang Z L, Pelton M, Fedin I, et al. A room temperature continuous-wave nanolaser using colloidal quantum wells. Nat Commun, 2017, 8, 143
[37] Lee J, Karnadi I, Kim J T, et al. Printed nanolaser on silicon. ACS Photonics, 2017, 4, 2117
[38] Li Y Z, Zhang J X, Huang D D, et al. Room-temperature continuous-wave lasing from monolayer molybdenum ditelluride integrated with a silicon nanobeam cavity. Nat Nanotech, 2017, 12, 987
[39] Jagsch S T, Triviño N V, Lohof F, et al. A quantum optical study of thresholdless lasing features in high-β nitride nanobeam cavities. Nat Commun, 2018, 9, 564
[40] He Z, Chen B, Hua Y, et al. CMOS compatible high-performance nanolasing based on perovskite-SiN hybrid integration. Adv Opt Mater, 2020, 8, 2000453
[41] Wu S F, Buckley S, Schaibley J R, et al. Monolayer semiconductor nanocavity lasers with ultralow thresholds. Nature, 2015, 520, 69
[42] Jacobsen R S, Andersen K N, Borel P I, et al. Strained silicon as a new electro-optic material. Nature, 2006, 441, 199
[43] Hochberg M, Baehr-Jones T, Wang G X, et al. Terahertz all-optical modulation in a silicon –polymer hybrid system. Nat Mater, 2006, 5, 703
[44] Soref R, Bennett B. Electrooptical effects in silicon. IEEE J Quantum Electron, 1987, 23, 123
[45] Qi B, Yu P, Li Y B, et al. Analysis of electrooptic modulator with 1-D slotted photonic crystal nanobeam cavity. IEEE Photon Technol Lett, 2011, 23, 992
[46] Javid M R, Miri M, Zarifkar A. Design of a compact high-speed optical modulator based on a hybrid plasmonic nanobeam cavity. Opt Commun, 2018, 410, 652
[47] Hendrickson J, Soref R, Sweet J, et al. Ultrasensitive silicon photonic-crystal nanobeam electro-optical modulator: Design and simulation. Opt Express, 2014, 22, 3271
[48] Shakoor A, Nozaki K, Kuramochi E, et al. Compact 1D-silicon photonic crystal electro-optic modulator operating with ultra-low switching voltage and energy. Opt Express, 2014, 22, 28623
[49] Jafari Z, Zarifkar A, Miri M, et al. All-optical modulation in a graphene-covered slotted silicon nano-beam cavity. J Lightwave Technol, 2018, 36, 4051
[50] Liu M, Yin X B, Zhang X. Double-layer graphene optical modulator. Nano Lett, 2012, 12, 1482
[51] Qiu C Y, Gao W L, Vajtai R, et al. Efficient modulation of 1.55 μm radiation with gated graphene on a silicon microring resonator. Nano Lett, 2014, 14, 6811
[52] Du W, Li E P, Hao R. Tunability analysis of a graphene-embedded ring modulator. IEEE Photon Technol Lett, 2014, 26, 2008
[53] Pan T, Qiu C Y, Wu J Y, et al. Analysis of an electro-optic modulator based on a graphene-silicon hybrid 1D photonic crystal nanobeam cavity. Opt Express, 2015, 23, 23357
[54] Liu H Q, Liu P G, Bian L A, et al. Electro-optic modulator side-coupled with a photonic crystal nanobeam loaded graphene/Al_2O_3 multilayer stack. Opt Mater Express, 2018, 8, 761
[55] Inoue S I, Otomo A. Electro-optic polymer/silicon hybrid slow light modulator based on one-dimensional photonic crystal waveguides. Appl Phys Lett, 2013, 103, 171101
[56] Yan H, Xu X C, Chung C J, et al. One-dimensional photonic crystal slot waveguide for silicon-organic hybrid electro-optic modulators. Opt Lett, 2016, 41, 5466
[57] Witmer J D, Hill J T, Safavi-Naeini A H. Design of nanobeam photonic crystal resonators for a silicon-on-lithium-niobate platform. Opt Express, 2016, 24, 5876
[58] Witmer J D, Valery J A, Arrangoiz-Arriola P, et al. High-*Q* photonic resonators and electro-optic coupling using silicon-on-lithium-niobate. Sci Rep, 2017, 7, 46313
[59] Fegadolli W S, Oliveira J E B, Almeida V R, et al. Compact and low power consumption tunable photonic crystal nanobeam cavity. Opt Express, 2013, 21, 3861
[60] Hadian Siahkal-Mahalle B, Abedi K. Ultra-compact low loss electro-optical nanobeam cavity modulator embedded photonic crystal. Opt Quant Electron, 2019, 51, 128
[61] Bolotin K I, Sikes K J, Jiang Z, et al. Ultrahigh electron mobility in suspended graphene. Solid State Commun, 2008, 146, 351
[62] Mak K F, Sfeir M Y, Wu Y, et al. Measurement of the optical conductivity of graphene. Phys Rev Lett, 2008, 101, 196405
[63] Yin Y W, Proietti R, Ye X H, et al. LIONS: An AWGR-based low-latency optical switch for high-performance computing and data centers. IEEE J Sel Top Quantum Electron, 2013, 19, 3600409
[64] Chen K, Singla A, Singh A, et al. OSA: an optical switching architecture for data center networks with unprecedented flexibility. IEEE/ACM Trans Networking, 2014, 22, 498
[65] Qiu C Y, Gao W L, Soref R, et al. Reconfigurable electro-optical directed-logic circuit using carrier-depletion micro-ring resonators. Opt Lett, 2014, 39, 6767
[66] Lira H L R, Manipatruni S, Lipson M. Broadband hitless silicon electro-optic switch for on-chip optical networks. Opt Express, 2009, 17, 22271
[67] Dong P, Liao S R, Liang H, et al. Submilliwatt, ultrafast and broadband electro-optic silicon switches. Opt Express, 2010, 18, 25225
[68] Zhou H Y, Qiu C Y, Xu Z Z, et al. A 2 $\times$ 2 silicon thermo-optic switch based on nanobeam cavities with ultra-small mode volumes. 2016 IEEE 13th International Conference on Group IV Photonics (GFP), 2016, 10
[69] Zhou H Y, Qiu C Y, Jiang X H, et al. Compact, submilliwatt, 2 $\times$ 2 sil-

icon thermo-optic switch based on photonic crystal nanobeam cavities. Photon Res, 2017, 5, 108
[70] Cheng Z W, Dong J J, Zhang X L. Ultracompact optical switch using a single semisymmetric Fano nanobeam cavity. Opt Lett, 2020, 45, 2363
[71] Soref R, Hendrickson J. Proposed ultralow-energy dual photonic-crystal nanobeam devices for on-chip $N \times N$ switching, logic, and wavelength multiplexing. Opt Express, 2015, 23, 32582
[72] Soref R, Hendrickson J R, Sweet J. Simulation of germanium nanobeam electro-optical 2 × 2 switches and 1 × 1 modulators for the 2 to 5 μm infrared region. Opt Express, 2016, 24, 9369
[73] Zhou H Y, Qiu C Y, Wu J Y, et al. 2 × 2 electro-optic switch with fJ/bit switching power based on dual photonic crystal nanobeam cavities. Conference on Lasers and Electro-Optics, 2016, JTh2A.105
[74] Bazin A, Lenglé K, Gay M, et al. Ultrafast all-optical switching and error-free 10 Gbit/s wavelength conversion in hybrid InP-silicon on insulator nanocavities using surface quantum wells. Appl Phys Lett, 2014, 104, 011102
[75] Dong G N, Deng W T, Hou J, et al. Ultra-compact multi-channel all-optical switches with improved switching dynamic characteristics. Opt Express, 2018, 26, 25630
[76] Meng Z M, Chen C B, Qin F. Theoretical investigation of integratable photonic crystal nanobeam all-optical switching with ultrafast response and ultralow switching energy. J Phys D, 2020, 53, 205105
[77] Liu Y, Qin F, Meng Z M, et al. All-optical logic gates based on two-dimensional low-refractive-index nonlinear photonic crystal slabs. Opt Express, 2011, 19, 1945
[78] Lengle K, Nguyen T N, Gay M, et al. Modulation contrast optimization for wavelength conversion of a 20 Gbit/s data signal in hybrid InP/SOI photonic crystal nanocavity. Opt Lett, 2014, 39, 2298
[79] Ji H, Galili M, Hu H, et al. 1.28-Tb/s demultiplexing of an OTDM DPSK data signal using a silicon waveguide. IEEE Photon Technol Lett, 2010, 22, 1762
[80] Dong G N, Wang Y L, Zhang X L. High-contrast and low-power all-optical switch using Fano resonance based on a silicon nanobeam cavity. Opt Lett, 2018, 43, 5977
[81] Meng Z M, Hu Y H, Wang C, et al. Design of high-Q silicon-polymer hybrid photonic crystal nanobeam microcavities for low-power and ultrafast all-optical switching. Photonics Nanostruct, 2014, 12, 83
[82] Asghari M, Krishnamoorthy A V. Energy-efficient communication. Nat Photon, 2011, 5, 268
[83] Pan J, Huo Y J, Yamanaka K, et al. Aligning microcavity resonances in silicon photonic-crystal slabs using laser-pumped thermal tuning. Appl Phys Lett, 2008, 92, 103114
[84] Eichenfield M, Camacho R, Chan J, et al. A picogram- and nanometre-scale photonic-crystal optomechanical cavity. Nature, 2009, 459, 550
[85] Li M, Pernice W H P, Tang H X. Tunable bipolar optical interactions between guided lightwaves. Nat Photon, 2009, 3, 464
[86] Gu L L, Jiang W, Chen X N, et al. Thermooptically tuned photonic crystal waveguide silicon-on-insulator Mach–Zehnder interferometers. IEEE Photon Technol Lett, 2007, 19, 342
[87] Espinola R L, Tsai M C, Yardley J T, et al. Fast and low-power thermooptic switch on thin silicon-on-insulator. IEEE Photon Technol Lett, 2003, 15, 1366
[88] Dong P, Qian W, Liang H, et al. Thermally tunable silicon racetrack resonators with ultralow tuning power. Opt Express, 2010, 18, 20298
[89] Zhang Y, He Y, Zhu Q M, et al. Single-resonance silicon nanobeam filter with an ultra-high thermo-optic tuning efficiency over a wide continuous tuning range. Opt Lett, 2018, 43, 4518
[90] Matsko A B. Practical applications of microresonators in optics and photonics. London: CRC Press, 2009
[91] Fan X D. Advanced photonic structures for biological and chemical detection. New York: Springer New York, 2009
[92] Sharma A, Xie S R, Zeltner R, et al. On-the-fly particle metrology in hollow-core photonic crystal fibre. Opt Express, 2019, 27, 34496
[93] Xiao Y F, Gong Q H. Optical microcavity: From fundamental physics to functional photonics devices. Sci Bull, 2016, 61, 185
[94] Zhi Y Y, Yu X C, Gong Q H, et al. Single nanoparticle detection using optical microcavities. Adv Mater, 2017, 29, 1604920
[95] Shao L B, Jiang X F, Yu X C, et al. Detection of single nanoparticles and lentiviruses using microcavity resonance broadening. Adv Mater, 2013, 25, 5616
[96] Li B B, Clements W R, Yu X C, et al. Single nanoparticle detection using split-mode microcavity Raman lasers. PNAS, 2014, 111, 14657
[97] Yang D Q, Wang A Q, Chen J H, et al. Real-time monitoring of hydrogel phase transition in an ultrahigh Q microbubble resonator. Photonics Res, 2020, 8, 497
[98] Yang D Q, Duan B, Liu X, et al. Photonic crystal nanobeam cavities for nanoscale optical sensing: A review. Micromachines, 2020, 11, 72
[99] Quan Q M, Floyd D L, Burgess I B, et al. Single particle detection in CMOS compatible photonic crystal nanobeam cavities. Opt Express, 2013, 21, 32225
[100] Rahman M G A, Velha P, de la Rue R M, et al. Silicon-on-insulator (SOI) nanobeam optical cavities for refractive index based sensing. Opt Sens Detect II, 2012, 8439, 84391Q
[101] Yao K Y, Shi Y C. High-Q width modulated photonic crystal stack mode-gap cavity and its application to refractive index sensing. Opt Express, 2012, 20, 27039
[102] Quan Q M, Burgess I B, Tang S K Y, et al. High-Q, low index-contrast polymeric photonic crystal nanobeam cavities. Opt Express, 2011, 19, 22191
[103] Xu P P, Yao K Y, Zheng J J, et al. Slotted photonic crystal nanobeam cavity with parabolic modulated width stack for refractive index sensing. Opt Express, 2013, 21, 26908
[104] Yang D Q, Kita S, Liang F, et al. High sensitivity and high Q-factor nanoslotted parallel quadrabeam photonic crystal cavity for real-time and label-free sensing. Appl Phys Lett, 2014, 105, 063118
[105] Kim S, Kim H M, Lee Y H. Single nanobeam optical sensor with a high Q-factor and high sensitivity. Opt Lett, 2015, 40, 5351
[106] Rodriguez G A, Markov P, Cartwright A P, et al. Photonic crystal nanobeam biosensors based on porous silicon. Opt Express, 2019, 27, 9536
[107] Gopinath A, Miyazono E, Faraon A, et al. Engineering and mapping nanocavity emission via precision placement of DNA origami. Nature, 2016, 535, 401
[108] Mandal S, Erickson D. Nanoscale optofluidic sensor arrays. Opt Express, 2008, 16, 1623
[109] Yang D Q, Wang C, Ji Y F. Silicon on-chip 1D photonic crystal nanobeam bandstop filters for the parallel multiplexing of ultra-compact integrated sensor array. Opt Express, 2016, 24, 16267
[110] Hagino H, Takahashi Y, Tanaka Y, et al. Effects of fluctuation in air hole radii and positions on optical characteristics in photonic crystal heterostructure nanocavities. Phys Rev B, 2009, 79, 085112
[111] Afzal F O, Halimi S I, Weiss S M. Efficient side-coupling to photonic crystal nanobeam cavities via state-space overlap. J Opt Soc Am B, 2019, 36, 585
[112] Liang F, Clarke N, Patel P, et al. Scalable photonic crystal chips for high sensitivity protein detection. Opt Express, 2013, 21, 32306
[113] Frank I W, Deotare P B, McCutcheon M W, et al. Programmable photonic crystal nanobeam cavities. Opt Express, 2010, 18, 8705
[114] Panettieri D, O'Faolain L, Grande M. Control of Q-factor in nanobeam cavities on substrate. 2016 18th International Conference on Transparent Optical Networks (ICTON), 2016, 1
[115] Xiong Y L, Wangüemert-Pérez J G, Xu D X, et al. Polarization splitter and rotator with subwavelength grating for enhanced fabrication tolerance. Opt Lett, 2014, 39, 6931

Daquan Yang received the B.S. degree in electronic information science and technology from the University of Jinan in 2005, and the Ph.D. degree in Information and Communication Engineering from Beijing University of Posts and Telecommunications in 2014, respectively. During his Ph. D., he joined the school of engineering and applied science at the Harvard University as a visiting follow for two years. Then, he joined the faculty of Beijing University of Posts and Telecommunications in 2014, and was promoted to an associate professor in 2016. He was awarded the Beijing Nova Program by Beijing Municipal Science and Technology Commission in 2020. His research interests include microcavity optics and micro-nano optical precision measurement.

Yunfeng Xiao received the B.S. and Ph.D. degrees in physics from University of Science and Technology of China in 2002 and 2007, respectively. After a postdoctoral research at Washington University in St. Louis, he joined the faculty of Peking University in 2009, and was promoted a tenured professor in 2014 a full professor in 2019. His research interests lie in the fields of whispering-gallery microcavity optics and photonics. He has authored or co-authored more than 170 refereed journal papers in Science, Nature Photonics, PNAS, PRL et al. He has delivered over 100 plenary/keynote/invited talks/seminars in international/national conferences/universities. He is an OSA Fellow, and has served as the committee for more than 30 international conferences.